



## ARTICLE OPEN

# Vaccine-induced antibodies target sequestered viral antigens to prevent ocular HSV-1 pathogenesis, preserve vision, and preempt productive neuronal infection

Derek J. Royer<sup>1</sup>, Joshua F. Hendrix<sup>1</sup>, Chelsea M. Larabee<sup>2</sup>, Alaina M. Reagan<sup>2</sup>, Virginie H. Sjoelund<sup>3</sup>, Danielle M. Robertson<sup>4</sup> and Daniel J. J. Carr<sup>1,5</sup>

The cornea is essential for vision yet highly sensitive to immune-mediated damage following infection. Generating vaccines that provide sterile immunity against ocular surface pathogens without evoking vision loss is therefore clinically challenging. Here, we tested a prophylactic live-attenuated vaccine against herpes simplex virus type 1 (HSV-1), a widespread human pathogen that can cause corneal blindness. Parenteral vaccination of mice resulted in sterile immunity to subsequent HSV-1 challenge in the cornea and suppressed productive infection of the nervous system. This protection was unmatched by a relevant glycoprotein subunit vaccine. Efficacy of the live-attenuated vaccine involved a T-dependent humoral immune response and complement C3 but not Fcγ-receptor 3 or interferon- $\alpha/\beta$  signaling. Proteomic analysis of viral proteins recognized by antiserum revealed an unexpected repertoire dominated by sequestered antigens rather than surface-exposed envelope glycoproteins. Ocular HSV-1 challenge in naive and subunit-vaccinated mice triggered vision loss and severe ocular pathologies including corneal opacification, scar formation, neovascularization, and sensation loss. However, corneal pathology was absent in mice receiving the live-attenuated vaccine concomitant with complete preservation of visual acuity. Collectively, this is the first comprehensive report of a prophylactic vaccine candidate that elicits resistance to ocular HSV-1 infection while fully preserving the cornea and visual acuity.

*Mucosal Immunology* \_\_\_\_\_; <https://doi.org/10.1038/s41385-019-0131-y>

## INTRODUCTION

Vaccine immunology research classically focuses on generating sterile immunity and identifying the mechanisms responsible for protection against infection. However, this approach is inadequate when considering pathogens that affect delicate organs and tissues such as the eye and nervous system. While the eye is well known as an immune-privileged organ, it remains highly susceptible to inflammatory damage. For this reason, many regulatory mechanisms temper ocular inflammation to preserve visual clarity.<sup>1–3</sup> Nonetheless, excessive inflammatory responses in the eye often break tolerance, contribute to permanent vision loss, and significantly impact quality of life.<sup>4–6</sup> Clinical management of ocular infections is often challenging and requires close attention to controlling both the pathogen and host inflammation to preserve the visual axis.<sup>7,8</sup> Accordingly, it is important to consider the potential of vaccine-induced inflammatory responses during the initial stages of vaccine development when targeting pathogens that commonly affect the eye.

Herpes simplex virus type 1 (HSV-1) is a widespread human pathogen that is of particular relevance to this topic. In addition to being a leading cause of infectious corneal blindness, HSV-1 is a clinically important cause of encephalitis and has recently emerged as the leading cause of primary genital herpes in

women of childbearing age in the USA.<sup>9–11</sup> The success of the pathogen lies in its ability to evade immune responses and establish latency in sensory neurons for the life of the host. Furthermore, the total reservoir of latent virus in the trigeminal ganglia (TG), which supply sensory innervation to orofacial mucosal sites, correlates with reactivation risk and clinical disease burden in animal models.<sup>12,13</sup> Chronic viral reactivation in the human eye is associated with a myriad of clinically important corneal pathologies including scarring, neovascularization, and persistent epithelial defects. Current therapies aim to suppress ocular inflammation with steroids and inhibit viral replication with nucleoside analog drugs, but such interventions do not “cure” the disease. Moreover, recurrences frequently persist even when on long-term, prophylactic treatment with these agents.<sup>8</sup> Visual morbidity can be so severe that corneal transplantation may be necessary to restore vision, although this remedy often has diminishing returns due to increased graft rejection rates.<sup>14</sup> Novel therapies to block HSV-1 pathogenesis are in development.<sup>15–17</sup> Considerable effort has also been applied to developing a therapeutic HSV vaccine to alleviate viral reactivation in patients with recurrent outbreaks.<sup>18–20</sup> However, we contend that prophylactic vaccination would be a highly effective strategy to prevent HSV-1-associated disease in the eye, skin, and nervous system.

<sup>1</sup>Department of Ophthalmology, University of Oklahoma Health Sciences Center, Oklahoma City, OK, USA; <sup>2</sup>Oklahoma Center for Neuroscience, University of Oklahoma Health Sciences Center, Oklahoma City, OK, USA; <sup>3</sup>Laboratory for Molecular Biology and Cytometry Research, University of Oklahoma Health Sciences Center, Oklahoma City, OK, USA; <sup>4</sup>Department of Ophthalmology, University of Texas Southwestern Medical Center, Dallas, TX, USA and <sup>5</sup>Department of Microbiology and Immunology, University of Oklahoma Health Sciences Center, Oklahoma City, OK, USA

Correspondence: Daniel J. J. Carr (Dan-Carr@ouhsc.edu)

Received: 28 March 2018 Accepted: 30 December 2018

Published online: 22 January 2019



Herein, we provide a comprehensive immunologic and ophthalmologic evaluation of the protective efficacy of a prophylactic live-attenuated vaccine for HSV-1. Although humans suffer ocular disease largely as a result of HSV-1 reactivation, immunologically naive mice develop robust, clinically relevant corneal disease following primary infection. Therefore, ocular HSV-1 infection in mice serves as a model to study the dynamics and mechanisms of prophylactic protection from the viewpoints of both viral pathogenesis and immune-mediated tissue damage. Using the eye as a clinically relevant site of HSV-1 infection following prophylactic vaccination, we show that a live-attenuated HSV-1 vaccine drives a T-dependent humoral immune response that elicits sterilizing immunity, limits the establishment of viral latency, and fully preserves the visual axis. Thorough characterization of the latter component is missing from nearly all previous efforts to characterize the “efficacy” of vaccines against ocular HSV-1 infection. Moreover, we identify that many dominant HSV-1 antibody targets are not exposed glycoproteins, but rather sequestered antigens only accessible within intracellular compartments. Our previous work shows that humoral immunity is essential for prophylactic protection against ocular HSV-1 infection through a mechanism involving the neonatal Fc receptor (FcRn) and intracellular complement fixation in outbred CD-1 mice.<sup>21,22</sup> The current investigation uses the genetic and immunologic tools available with the inbred C57BL/6 strain to build upon our previous studies.

## METHODS

### Mice and immunization scheme

Inbred C57BL/6 WT (stock # 000664), TCR $\alpha^{-/-}$  (stock # 002116),  $\mu$ MT (stock # 002288), Fc $\gamma$ RIII $^{-/-}$  (stock # 003171), C3 $^{-/-}$  (stock # 003641), and Ai14/Rosa26-tdTomato Cre-reporter (stock # 007914) mice were obtained from the Jackson Laboratory (Bar Harbor, ME). *Irfnar1<sup>-/-</sup>* mice were bred in house. All animals were housed in specific-pathogen free conditions at the Dean McGee Eye Institute. This study was conducted according to protocols approved by the University of Oklahoma Health Sciences Center animal care and use committee. Mice were anesthetized for all invasive procedures by i.p. injection of ketamine (100 mg/kg) plus xylazine (6.6 mg/kg) and were euthanized by cardiac perfusion with 10 ml PBS for tissue collection. Animals were immunized using a prime-boost regimen via ipsilateral footpad (subcutaneous) and hind flank (intramuscular) injections 3 weeks later as previously described.<sup>21</sup> Briefly, the immunization dosage for the live-attenuated virus was  $1 \times 10^5$  PFU of HSV-1  $\Delta$ NLS in 10  $\mu$ L PBS (primer and boost). The subunit vaccine included 2.5  $\mu$ g of recombinant truncated gD from HSV-2 adjuvanted with 25  $\mu$ l Imject alum (Thermo Scientific) and 10  $\mu$ g monophosphoryl lipid A from *Salmonella enterica* serovar Minnesota (Sigma) in a 35- $\mu$ l total volume (primer and boost). Animals were 6–10 weeks old upon primary immunization and were ocularly challenged with HSV-1 30 days following the secondary boost. Serum neutralization titers were determined prior to challenge and reflect reciprocal serum dilutions upon 50% reduction of cytopathic effect at 24 h using the median tissue culture infectious dose (TCID<sub>50</sub>) for HSV-1 McKrae in Vero cell monolayers as previously reported.<sup>21</sup>

### Virus strains and ocular infection

As previously documented,<sup>21–23</sup> the HSV-1  $\Delta$ NLS vaccine is a live-attenuated recombinant virus derived from the HSV-1 KOS strain; the vaccine strain is rendered attenuated by deletion of the nuclear localization signal on the virally-encoded *ICP0* gene. Unless otherwise indicated, all mice were ocularly challenged with  $1 \times 10^4$  PFU HSV-1 McKrae per eye following partial epithelial debridement of the cornea. Ai14/Rosa26-tdTomato reporter mice were ocularly infected with  $1 \times 10^3$  PFU of transgenic HSV-1 (SC16 strain) expressing Cre recombinase to visualize productively

infected cells in cryosectioned TG by confocal microscopy.<sup>24</sup> Virus stocks were propagated and maintained in high-titer aliquots as previously described.<sup>21,24,25</sup>

### Assessments of viral pathogenesis

Titers of infectious virus were determined in clarified tissue homogenates by standard plaque assay on monolayers of Vero cells (American Type Culture Collection). Viral lytic gene expression and analysis of latent HSV-1 was evaluated by PCR as previously described.<sup>22</sup> Briefly, DNA was isolated from TGs at day 30 p.i. and subjected to quantitative PCR for HSV-1 genome using a proprietary primer-probe copy number kit (Primer Design). For relative expression of HSV-1 genes (LAT, TK, ICP27), tissue was harvested at the indicated times p.i. for RNA purification, cDNA conversion, and viral transcript expression was evaluated by real-time PCR. Antiviral gene expression was measured by real-time PCR using PrimePCR technology (Biorad).

### Antibody repertoire analysis

To analyze the repertoire of viral proteins recognized by HSV-1  $\Delta$ NLS antiserum,  $4 \times 10^5$  Vero cells were plated in each well of a 6 well plate and infected with  $4 \times 10^5$  PFU HSV-1 McKrae (MOI = 1.0). At 18 h p.i., cells were collected, washed in PBS, and pelleted by centrifugation at  $300 \times g$  for 5 min. Pellets were re-suspended in 500  $\mu$ l of 1% Triton-X100 detergent in PBS (cell lysis buffer) to lyse cells, vortexed every 5 min and placed on ice for a total of 15 min. Cell lysates were clarified by centrifugation at  $10,000 \times g$  for 10 min. Next, supernatants from infected and uninfected Vero cells were mixed with 4  $\mu$ l of serum from naive or immunized mice and 100  $\mu$ l of immunomagnetic protein G microbeads (Miltenyi Biotec) and incubated at 4°C for 30 min. Microbead/antibody/protein complexes were then immobilized in  $\mu$ MACS magnetic columns (Miltenyi Biotec). After thorough column washing with cell lysis buffer, retained proteins were eluted with 500  $\mu$ l of 100 mM glycine, pH 2.5 and stored at 4°C. Tryptic digests were prepared and analysed by liquid chromatography-tandem mass spectrometry (LC-MS/MS) to identify viral proteins as described in the supplementary methods.

### Flow cytometry, adoptive transfers, and in vivo receptor neutralization

Spleens were harvested and single cell suspensions created by filtration through 70  $\mu$ m mesh in RPMI1640 culture media containing 10% fetal bovine serum and antibiotics. Splenocytes were pelleted and erythrocytes lysed using 0.84% NH<sub>4</sub>Cl (J.T. Baker) in H<sub>2</sub>O. For T cell repertoire profiling, splenocytes were labeled with anti-CD45, anti-CD3, and anti-CD8 antibodies (eBioscience) and MHC class I K<sup>b</sup> tetramers provided by the NIH Tetramer Core Facility for identification of HSV-1 specific CD8<sup>+</sup> T cells. Tetramer-labeled cells were analyzed using a MacsQuant flow cytometer (Miltenyi Biotec) as previously described.<sup>23</sup> For adoptive transfers into *Irfnar1<sup>-/-</sup>* mice, bulk preparations of CD3<sup>+</sup> splenocytes were obtained by immunomagnetic isolation using anti-CD3 microbeads (Miltenyi Biotec) according to the manufacturer's directions. Alternatively, splenocytes were labeled with anti-CD4 or anti-CD8 antibodies (eBioscience) and sorted using an S3e cell sorter (Biorad) for adoptive transfers into TCR $\alpha^{-/-}$  mice. Adoptive transfer of isolated cells was mediated by intravenous retroorbital injection. In some experiments, TCR $\alpha^{-/-}$  mice were injected i.p. with 250  $\mu$ g anti-mouse CD154 (MR1 clone) or Armenian hamster IgG isotype (both from BioXcell) at days 0, 3, and 6 p.i. to evaluate CD40-dependent immune activation following adoptive transfer of CD4 T cells.

### Corneal Pathology

Corneolimbic buttons were harvested from eyes at day 30 p.i., fixed in 4% paraformaldehyde, and permeabilized in 1% Triton-

X100 in PBS to facilitate imaging. Corneas were subsequently labeled with antibodies for Lyve1 and CD31 (Millipore) and flat-mounted for analysis of neovascularization using an Olympus FV1200 laser scanning confocal microscope and 10x objective, as described.<sup>21</sup> The total area positive for vasculature per field of view (4 quadrants/cornea) was quantified using Metamorph software (Molecular Devices, Inc.). Alternatively, corneas were assessed for collagen remodeling via multiphoton SHG microscopy using a Leica SP8 confocal microscope equipped with an ultrafast Ti:Sapphire multiphoton Laser (Coherent Chameleon Vision II) as described.<sup>26</sup> Briefly, images were generated using an 880 nm wavelength excitation beam on corneolimbic buttons suspended in 35 mm glass-bottom dishes (MatTek Corp.) containing 50% glycerol in PBS. Resultant forward and backward SHG signal images from the central cornea were acquired using a 25x water immersion objective lens. Image stacks were qualitatively evaluated for collagen remodeling using a 3-tier scale to reflect normal structure, small regional defects, or widespread scarring. Ranks were empirically determined using images from healthy and scarred corneas for reference. Additionally, a masked clinician monitored corneal opacity using a Kowa SL14 portable slit lamp biomicroscope. Opacification was rated on a scale of 1–6, where 1 indicates stromal haze, 2 indicates moderate opacity, 3 indicates moderate opacity with regional dense opacity, 4 indicates diffuse opacity, and 5 indicated diffuse dense opacity with corneal ulcer as described previously.<sup>21</sup> Corneal mechanosensation was measured using a handheld Cochet-Bonnet esthesiometer to assess blink reflexes in alert mice (Luneau Technology). Spatial visual acuity was monitored by optokinetic tracking (OKT) behavioral responses using an OKT apparatus and Optometry software (Cerebral Mechanics, Inc.) as described.<sup>27,28</sup> Briefly, masked observers monitored animals centered in a virtual 3D environment for head turning behavior in response to varying frequencies of rotating vertical lines. Visual acuity for left and right eyes is represented by the highest frequency for which animals track clockwise and counter-clockwise line rotation, respectively.

#### Statistical analysis

Graphpad Prism 5 was used for statistical analysis. Unless indicated otherwise, data shown reflect means  $\pm$  standard errors of the means. Statistical tests utilized for data analysis are described in each figure legend. Thresholds for significant findings are denoted as: \* $P < 0.05$ ; \*\* $P < 0.01$ ; and \*\*\* $P < 0.001$  in each figure.

## RESULTS

The HSV-1 0ΔNLS vaccine requires B and T cells but not IFN $\alpha/\beta$  signaling for prophylactic protection against HSV-1 neurovirulence. The immunologic compartments required for prophylactic protection against ocular HSV-1 infection were investigated using wildtype (WT) and immune-deficient C57BL/6 mice immunized with a previously characterized live-attenuated virus termed "HSV-1 0ΔNLS"<sup>21–23</sup> or a glycoprotein D (gD-2) subunit vaccine similar in composition to the GSK Herpevac HSV-2 vaccine that demonstrated partial cross-reactive efficacy against genital HSV-1 infection in human clinical trials.<sup>10,29</sup> Regardless of which vaccine was administered, protection against ocular HSV-1 challenge in mice required both B and T cells, as B cell deficient ( $\mu$ MT) mice and T cell receptor alpha chain-deficient (TCR $\alpha^{-/-}$ ) mice lacked detectable virus-neutralizing antibody following immunization and succumbed to encephalitis following ocular HSV-1 challenge (Fig. 1a). While the gD-2 subunit vaccine confers modest protection against HSV-1 in outbred CD-1 mice,<sup>21,22</sup> it elicited no protection in the C57BL/6 strain in terms of post-challenge survival relative to naive controls (Fig. 1a). Consistent with this observation, the gD-2 subunit failed to elicit serum-neutralizing titers in

C57BL/6 mice beyond the detection threshold (Fig. 1b). In contrast, all WT and IFN $\alpha/\beta$  receptor-deficient ( $lfnar1^{-/-}$ ) animals immunized with HSV-1 0ΔNLS survived the challenge (Fig. 1a). Vaccine-mediated protection in  $lfnar1^{-/-}$  mice was unexpected (Fig. 1a) given the central role of IFN $\alpha/\beta$  in acute antiviral defense against HSV-1.<sup>30–33</sup> Immunologically naive mice (WT and  $lfnar1^{-/-}$ ) lacked detectable neutralizing antibody to HSV-1 prior to challenge. However, protection in HSV-1 0ΔNLS-vaccinated  $lfnar1^{-/-}$  mice was associated with high pre-challenge serum neutralization titers (Fig. 1b).

The pathogenesis of HSV-1 in naive hosts involves primary infection at mucosal sites with subsequent spread to tissue-innervating sensory nerves where the virus persists indefinitely. To determine the prophylactic impact of each vaccine on acute viral pathogenesis, HSV-1 titers were measured following ocular challenge in the tear film, cornea, and trigeminal ganglia (TG)—the sensory ganglion that supplies innervation to orofacial mucosal sites. Viral shedding was eliminated in the tears of HSV-1 0ΔNLS-vaccinated WT mice by days 3–5 post infection (p.i.), although shedding was sustained through day 5 in all other groups (Fig. 1c). The HSV-1 0ΔNLS vaccine facilitated a 5-log reduction in viral shedding in the tear film of immunized  $lfnar1^{-/-}$  mice relative to naive controls (Fig. 1c). Viral titers were also reduced in corneas from HSV-1 0ΔNLS-immunized WT and  $lfnar1^{-/-}$  mice compared to their respective naive counterparts (Fig. 1d, left). Moreover, infectious virus was not detected in the TG of HSV-1 0ΔNLS-immunized WT or  $lfnar1^{-/-}$  mice at day 5 p.i. (Fig. 1d, right). In contrast, HSV-1 disseminated to the TG of HSV-1 0ΔNLS-immunized  $\mu$ MT mice (Fig. 1e) suggesting that antibody abrogates viral neurovirulence.

Viral neuroinvasion and latency were subsequently investigated using highly sensitive molecular genetic approaches. First, HSV-1 DNA was analyzed by quantitative PCR in the TG of challenged animals at day 30 p.i., a time-point when viral latency is stably established.<sup>34</sup> Both WT and  $lfnar1^{-/-}$  mice immunized with HSV-1 0ΔNLS had up to 1000 times fewer HSV-1 genome copies than surviving naive or gD-2-immunized WT animals (Fig. 2a). Virus-encoded latency associated transcripts (LAT) epigenetically regulate neuronal latency.<sup>35</sup> Therefore, LAT expression was measured at day 30 p.i. by semiquantitative RT-PCR as a secondary correlate of total latent HSV-1 in the TG. LAT expression was markedly less in TG from HSV-1 0ΔNLS-immunized WT mice compared to gD-2-immunized or naive controls (Fig. 2b). Although the HSV-1 0ΔNLS vaccine limited neuroinvasion and the total amount of latent virus, vaccination did not completely preempt infection of nerve ganglia. Therefore, whether latent virus detected in animals vaccinated with HSV-1 0ΔNLS reflected productive or abortive neuronal infection remained to be determined.<sup>35</sup> Accordingly, a dually transgenic model system was utilized to identify nerves with a history of productive HSV-1 infection. For these studies, mice encoding a ubiquitous Cre-inducible tdTomato fluorescent reporter construct were challenged with transgenic HSV-1 encoding Cre recombinase under the infected cell protein ICP0 lytic gene promoter.<sup>24</sup> In this system, any surviving cell with a history of viral lytic gene (ICP0) activity will express tdTomato. Trigeminal ganglia from naive and HSV-1 0ΔNLS-vaccinated reporter mice were harvested at day 30 p.i., cryo-sectioned, and imaged by confocal microscopy. Reporter-expressing cells (tdTomato<sup>+</sup>) were abundant in TG from naive animals but conspicuously absent in TG from HSV-1 0ΔNLS-vaccinated mice following ocular challenge (Fig. 2c). Taken together, our data indicate that the HSV-1 0ΔNLS vaccine drives a T-dependent humoral immune response that rapidly clears HSV-1 from the cornea, impedes neuroinvasion, and blocks productive infection of peripheral nerves following challenge. However, the molecular and cellular mechanisms that mediate protection remained to be determined.



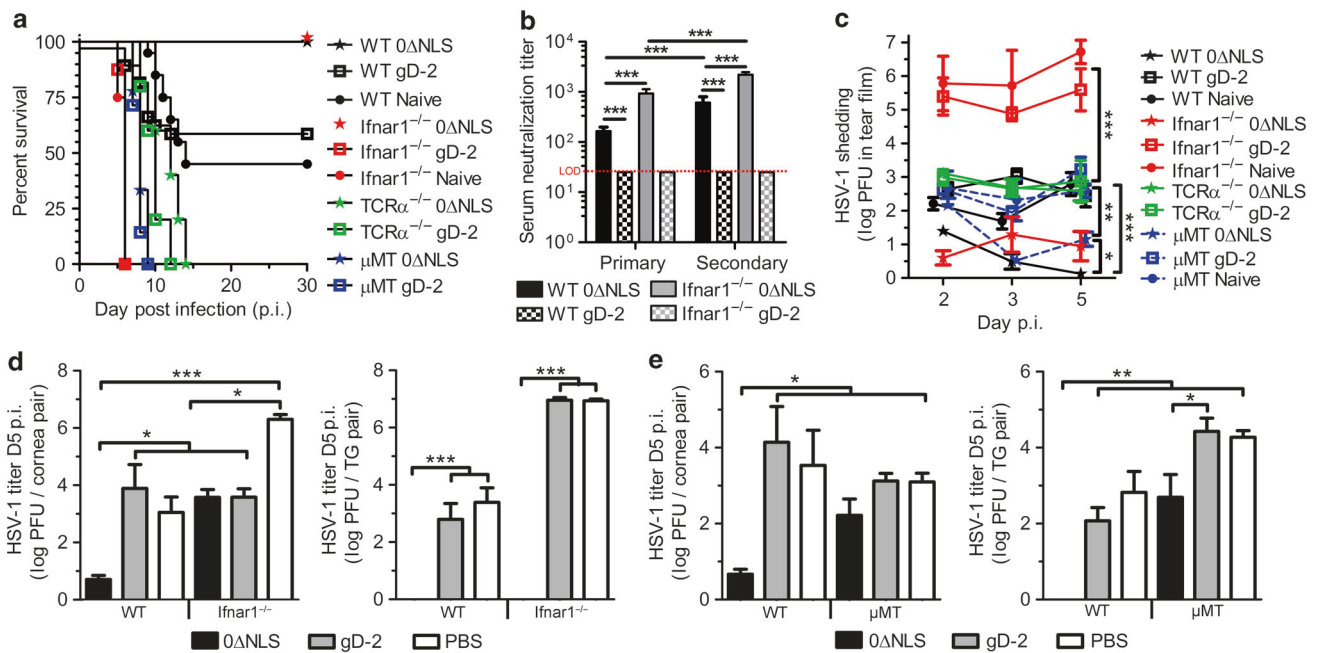


**Fig. 1** Immunologic compartments required for prophylactic protection against ocular HSV-1 challenge. Naive and prophylactically immunized C57BL/6 mice were ocularly infected with  $1 \times 10^4$  PFU HSV-1 McKrae per eye to assess efficacy of the live-attenuated HSV-1 0ΔNLS vaccine and a gD-2 subunit vaccine. **a** Survival proportions of naive and vaccinated WT, Ifnar1<sup>-/-</sup>, μMT, and TCRα<sup>-/-</sup> mice ( $n \geq 20$  WT, 8 Ifnar1<sup>-/-</sup>, 7 μMT, 5 TCRα<sup>-/-</sup> per group with  $\geq 2$  independent experiments). **b** Serum neutralization titers in WT and Ifnar1<sup>-/-</sup> mice at 21–30 days following primary and secondary immunization with HSV-1 0ΔNLS or the gD-2 subunit ( $n \geq 8$  mice/group; 2 independent experiments). Data reflect the reciprocal serum dilution upon which a 50% reduction in tissue culture cytopathic effect was observed. Neutralization titers were not detected ( $<1:25$ ) in immunized μMT and TCRα<sup>-/-</sup> animals. **c** Viral shedding in the tear film of vaccinated and naive mice at days 2, 3, and 5 p.i. ( $n = 4–11$  vaccinated mice/group,  $n = 2$  naive μMT and Ifnar1<sup>-/-</sup> controls; 2–3 independent experiments). **d** HSV-1 titers in the corneas and trigeminal ganglia (TG) of WT and Ifnar1<sup>-/-</sup> mice at day 5 p.i. ( $n = 3–10$  mice/group; 2–3 independent experiments). **e** HSV-1 titers in the corneas and TG of WT and μMT mice at day 5 p.i. ( $n = 4–7$  mice/group,  $n = 2$  naive μMT controls; 2–3 independent experiments). Data in panels **b**, **d**, and **e** were analyzed by one-way ANOVA with Newman-Keuls multiple comparisons tests; data in panel **c** was analyzed by two-way ANOVA with Bonferroni post-tests

The mechanisms underlying protection in HSV-1 0ΔNLS-vaccinated Ifnar1<sup>-/-</sup> mice were explored further during the acute stage of infection. We have previously shown that FcRn and implicitly intracellular antibody is requisite for ocular protection against HSV-1 challenge in prophylactically vaccinated mice.<sup>22</sup> Because intracellular antibody-pathogen complexes can initiate NFκB, AP-1, and IRF-dependent inflammatory responses,<sup>36</sup> we sought to determine whether prophylactic immunity could modulate autophagy-associated or interferon-stimulated gene (ISG) expression in the cornea independent of IFNα/β receptor signaling. Vaccination generated strong serum neutralizing antibody responses ( $>1:1000$ ) and limited corneal edema in Ifnar1<sup>-/-</sup> mice following challenge (Figs. 3a, b). Viral replication indicated by *thymidine kinase* (*TK*) expression was reduced substantially in the corneas of HSV-1 0ΔNLS-vaccinated Ifnar1<sup>-/-</sup> mice relative to naive Ifnar1<sup>-/-</sup> controls at 48 h p.i. (Fig. 3c). Moreover, *TK* expression in the corneas of HSV-1 0ΔNLS-vaccinated Ifnar1<sup>-/-</sup> mice was similar to levels observed in naive WT controls (Fig. 3c). However, unlike naive WT controls, no viral *TK* expression was detected in TG from HSV-1 0ΔNLS-vaccinated Ifnar1<sup>-/-</sup> mice (Fig. 3d). This data further supports our finding that vaccination with HSV-1 0ΔNLS prevents productive neuronal infection. Antibody-dependent, Ifnar1-independent signaling did not modulate host antiviral gene expression in the corneas of vaccinated Ifnar1<sup>-/-</sup> mice aside from upregulation of tetherin (*Bst2*), inducible nitric oxide synthase (*Nos2*), and MHC class-I (*H2-K1*) with concomitant suppression of IL-1β (Figs. 2e, f). Nonetheless, prophylactic protection elicited by HSV-1 0ΔNLS compensates for a complete loss of the antiviral IFNα/β receptor-signaling pathway.

Cell-mediated immunity conferred by the HSV-1 0ΔNLS vaccine offers inadequate protection against viral pathogenesis in the absence of antibody. Over the past decade, the HSV vaccine research community has keenly focused on memory T cell responses as a component of prophylactic protection.<sup>37–39</sup> While cell-mediated immunity is essential for control of HSV-1 in naive hosts, the extent to which primed T cells contribute to prophylactic protection against HSV-1 remains unclear. Because CD8 T cells maintain HSV-1 latency in the TG,<sup>40</sup> we first assessed the CD8 T cell repertoire in immunized mice using MHC class-I tetramers reflecting the top three immunodominant HSV-1 epitopes in C57BL/6 mice.<sup>41</sup> By day 5 p.i., the systemic pool of tetramer-specific CD8 T cells surveyed in the spleen was no different among naive, gD-2-immunized, or HSV-1 0ΔNLS-immunized WT mice (Fig. 4a). Given the modest reduction in HSV-1 titers measured in TG from HSV-1 0ΔNLS-vaccinated μMT mice compared to those receiving the gD-2 subunit (Fig. 1e), we also surveyed the HSV-specific CD8 T cell repertoire in μMT mice. However, the HSV-specific CD8 T cell repertoire in μMT mice was similar to that measured in WT and, likewise, was not appreciably impacted by vaccination (Fig. S1). In a previous investigation using outbred CD-1 mice, we identified increased acute T cell infiltration into the corneas of HSV-1 0ΔNLS-immunized animals relative to naive controls at day 5 p.i.<sup>21</sup> Importantly, corneal T cell infiltration is associated with tissue pathology and visual morbidity over time.<sup>42–44</sup> Therefore, prophylactic vaccination might enhance effector T cell responses in infected tissues without expanding the repertoire of HSV-specific T cells. Although early enhancement of corneal T cell infiltration was observed in HSV-1 0ΔNLS-vaccinated animals,<sup>21</sup>

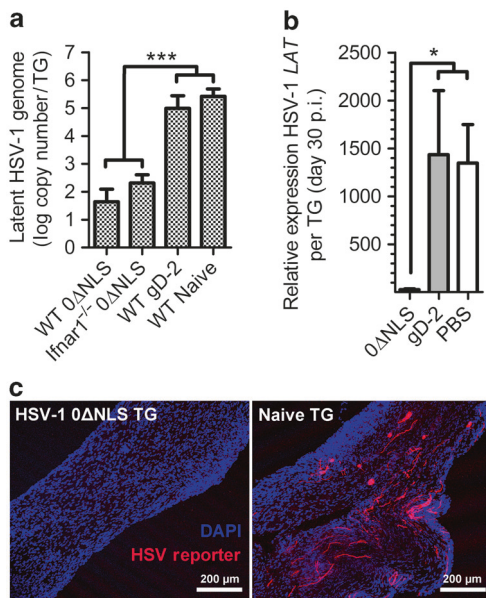


**Fig. 2** Impact of prophylactic vaccination on HSV-1 latency. Latent virus was assessed in trigeminal ganglia from vaccinated and naive mice following ocular infection with  $1 \times 10^4$  PFU HSV-1 McKrae per eye. **a** Quantitative PCR reads of HSV-1 genome copy numbers in the TG of surviving WT and *Ifnar1*<sup>-/-</sup> mice at day 30 p.i. ( $n = 6-7$  mice per group; 2-3 independent experiments). **b** Relative expression of HSV-1 latency associated transcript (*LAT*) in the TG of surviving WT mice at day 30 p.i. ( $n = 4-6$  mice/group; 2 independent experiments). Reported *LAT* expression is relative to *phosphoglycerate kinase 1* expression and normalized to uninfected controls. **c** Naive and vaccinated reporter mice expressing Cre-inducible tdTomato reporter construct on the *Rosa26* locus were ocularly challenged with  $1 \times 10^3$  PFU of transgenic HSV-1 expressing Cre-recombinase (SC16 strain) per eye. In this model, cells productively infected by HSV-1 express the tdTomato reporter. Confocal images of sectioned TGs from vaccinated and naive reporter mice at day 30 p.i. showing productively infected neurons exclusively in naive animals (images are representative of TG from 3 mice/group; 2 independent experiments; scale bar = 200  $\mu$ m). Data in panels **a** and **b** were analyzed by one-way ANOVA with Newman-Keuls multiple comparisons tests

findings from our lab show that the number of cornea-infiltrating/resident T cells remains steady over time in vaccinated CD-1 mice ( $399 \pm 101$  CD3<sup>+</sup> cells per cornea pair at day 30 p.i.). In contrast, corneas from naive CD-1 mice contain ten times as many T cells at day 30 p.i. ( $4069 \pm 1392$  CD3<sup>+</sup> cells per cornea pair;  $p < 0.05$ , *T*-test).

Bulk transfer of HSV-specific T cells has been shown to mediate a modest reduction in HSV-1 titers in the nervous system of naive *Ifnar1*<sup>-/-</sup> mice.<sup>31,45</sup> Accordingly, adoptive transfer experiments were performed to further characterize the contributions of T cells in prophylactic immunity to HSV-1 in the absence of preexisting humoral immunity. Initially,  $1 \times 10^6$  CD3<sup>+</sup> cells from the spleens of naive or HSV-1 0ΔNLS-immunized WT mice were transferred into naive *Ifnar1*<sup>-/-</sup> mice at the time of ocular challenge. Regardless of cell transfer source, all *Ifnar1*<sup>-/-</sup> mice exhibited signs of HSV-1 encephalitis by day 5 p.i. Consistent with this observation, the transferred cells had no impact on viral replication or dissemination (Figs. 4b, c).

We next evaluated the prophylactic impact of T cells by transferring  $1 \times 10^5$  CD4, CD8, or CD4 and CD8 T cells from the spleens of HSV-1 0ΔNLS-immunized WT mice into *TCR $\alpha$* <sup>-/-</sup> mice. Transfer of only CD4 or CD4 and CD8 T cells promoted survival in a fraction of *TCR $\alpha$* <sup>-/-</sup> mice following ocular HSV-1 challenge (Fig. 4d). All surviving *TCR $\alpha$* <sup>-/-</sup> mice had detectable levels of

serum neutralizing antibody at day 30 p.i. (Fig. 4e), yet the corneas of surviving mice exhibited gross pathologic opacification. Parallel experiments showed that while T cells from vaccinated WT mice facilitated subtle reductions in HSV-1 titers in the TG of *TCR $\alpha$* <sup>-/-</sup> mice, adoptive transfer did not abrogate viral dissemination to the central nervous system during acute infection (Fig. 4f). Given that the presence of virus-neutralizing antibody responses were linked to survival in our adoptive transfer model (Fig. 4e), we subsequently combined CD4 T cell transfers into *TCR $\alpha$* <sup>-/-</sup> mice with in vivo neutralization of CD154/CD40L to limit T cell-dependent B cell activation.<sup>46</sup> The low survival proportion of *TCR $\alpha$* <sup>-/-</sup> mice following adoptive transfer of CD4 T cells was lost upon neutralizing CD154 regardless of whether the CD4 T cells originated from naive or immunized WT mice (Fig. 4g). This difference was statistically significant for recipients of naive CD4 cells treated with IgG vs. anti-CD154 ( $p < 0.01$ , Mantel-Cox). Taken together, our data illustrate that primed effector T cells are likely minor contributors to prophylactic protection against HSV-1 infection following vaccination with HSV-1 0ΔNLS. Moreover, the diminutive protection that CD4 T cells provided to *TCR $\alpha$* <sup>-/-</sup> mice in terms of animal survival might be attributed to CD154-dependent promotion of antibody responses.

Humoral immunity elicited by HSV-1 0ΔNLS requires complement C3 but not Fc $\gamma$ RIII for optimal protection against viral neuroinvasion and latency

We have previously shown that acute viral clearance from the tear film of HSV-1 0ΔNLS vaccinated animals is mediated by complement C3 and not Fc $\gamma$  receptor 3 (Fc $\gamma$ RIII) following ocular HSV-1 challenge.<sup>22</sup> To substantiate the effector mechanisms responsible for humoral protection in the cornea and nerve ganglia, HSV-1 pathogenesis was evaluated further in immunized C3<sup>-/-</sup> and Fc $\gamma$ RIII<sup>-/-</sup> mice. All vaccinated animals exhibited similar pre-challenge serum neutralization titers<sup>22</sup> and survived the ocular challenge (Fig. 5a). In terms of latent viral burden at day 30 p.i., HSV-1 0ΔNLS-vaccinated Fc $\gamma$ RIII<sup>-/-</sup> mice were no more susceptible than vaccinated WT mice (Fig. 5b). In contrast, the amount of latent viral DNA detected in vaccinated C3<sup>-/-</sup> mice was comparable to naive controls (Fig. 5b).

In order to determine if the dynamics of viral clearance may ultimately impact the magnitude of viral latency, we subsequently assessed viral replication in naive and vaccinated C3<sup>-/-</sup> mice during acute infection. Viral lytic gene expression was elevated in corneas from HSV-1 0ΔNLS-vaccinated C3<sup>-/-</sup> mice relative to vaccinated WT mice by 24 h p.i. (Fig. 5c). By day 3 p.i., lytic gene expression was reduced in corneas and TG from HSV-1 0ΔNLS-vaccinated WT and C3<sup>-/-</sup> mice relative to their naive counterparts (Figs. 5d, e). However, there was a trend ( $p = 0.15$ ) in higher viral lytic gene expression in TG from vaccinated C3<sup>-/-</sup> animals compared to vaccinated WT (Fig. 5e). Infectious virus was cleared from the corneas of HSV-1 0ΔNLS-vaccinated WT and C3<sup>-/-</sup> mice by day 5 p.i. (Fig. 5f). Viral titers were also substantially reduced in the TG of vaccinated C3<sup>-/-</sup> mice compared to naive controls at day 5 p.i. (Fig. 5g). Nonetheless, low levels of infectious HSV-1 were detected in TG from some HSV-1 0ΔNLS-vaccinated C3<sup>-/-</sup> mice at day 5 p.i. (Fig. 5g). Taken together, our data indicate that C3 is categorically essential not only for efficient viral clearance at the point of mucosal exposure<sup>22</sup> but also for shielding against the establishment of neuronal latency in animals prophylactically vaccinated with HSV-1 0ΔNLS.

The HSV-1 0ΔNLS vaccine elicits antibody responses against heterogeneous viral proteins

Nearly all HSV vaccines tested in clinical trials to date have attempted to elicit humoral responses against exposed virion envelope glycoproteins.<sup>11,19,47</sup> We have previously shown that HSV-1 0ΔNLS antiserum recognizes a broad array of HSV-1 proteins by western blot.<sup>21</sup> Here, mass spectrometry was utilized

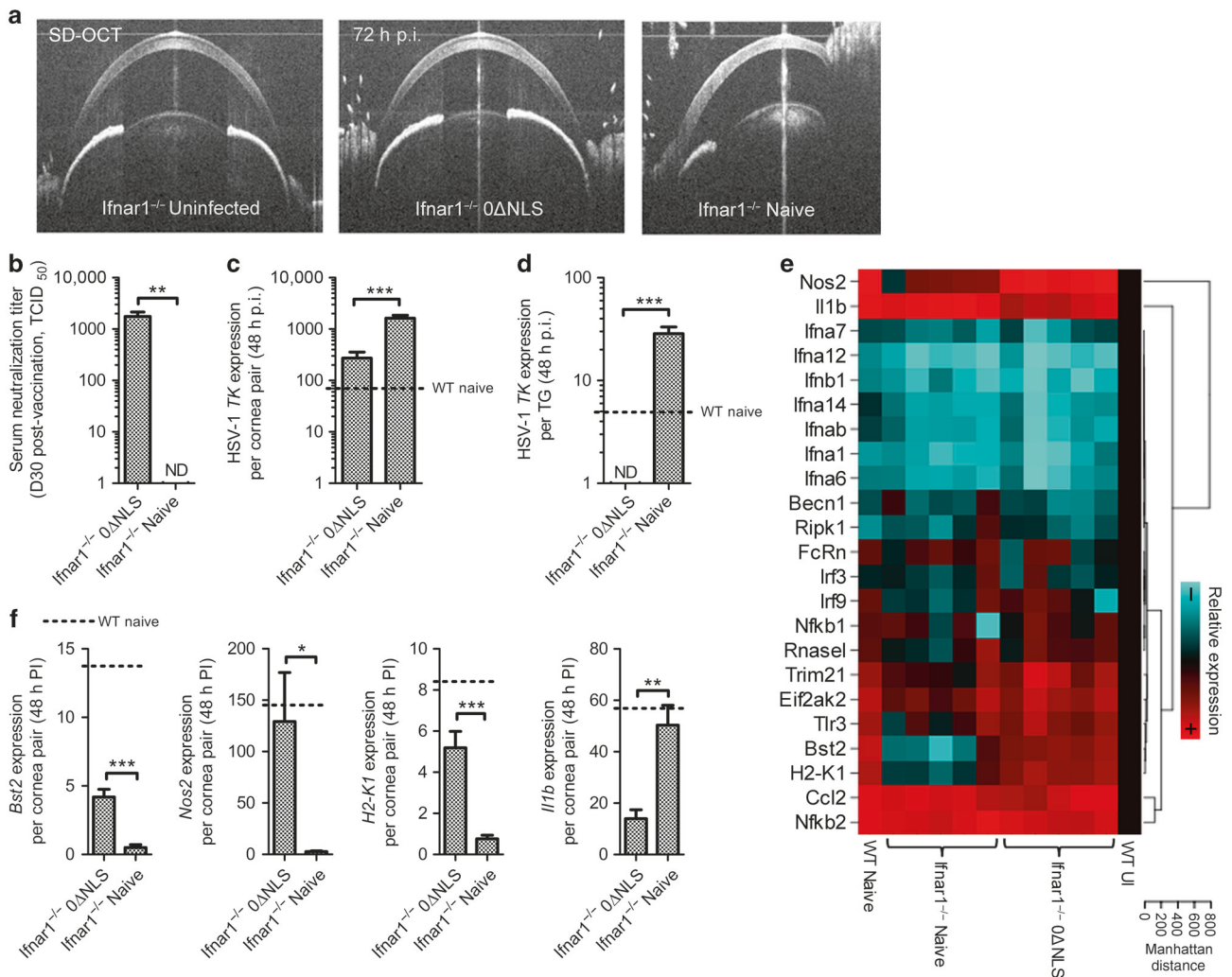


**Fig. 3** Contributions of type 1 interferon signaling to prophylactic protection. Type 1 interferon (IFN $\alpha/\beta$ ) receptor-deficient (*Ifnar1*<sup>-/-</sup>) mice were prophylactically vaccinated in the footpad with  $1 \times 10^5$  plaque forming units (PFU) of HSV-1 0 $\Delta$ NLS and ocularly challenged 30 days later with  $1 \times 10^5$  PFU HSV-1 McKrae per eye. **a** Spectral domain optical coherence tomography (SD-OCT) imaging of the anterior eye of *Ifnar1*<sup>-/-</sup> animals 72 h p.i. **b** Serum neutralizing titers in vaccinated and naive *Ifnar1*<sup>-/-</sup> mice. Relative expression of HSV-1 thymidine kinase (TK) in the cornea (**c**) and trigeminal ganglia (**d**) of *Ifnar1*<sup>-/-</sup> mice at 48 h post-infection (p.i.). Expression data was normalized to *glyceraldehyde 3-phosphate dehydrogenase* (GAPDH) expression and relative to tissue from uninfected WT C57BL/6 mice. **e** Heat map of antiviral gene expression at 48 h p.i. generated using Biorad PrimePCR technology and the National Cancer Institute's online Cluster Image Map tool (<http://discover.nci.nih.gov/cimminer/>). Host gene expression was relative to the geometric mean of *beta actin*, *GAPDH*, and *phosphoglycerokinase 1* expression and normalized to tissue from uninfected WT C57BL/6 mice. Data sets in which significant differences (Student's T tests) were identified in host gene expression between naive and vaccinated *Ifnar1*<sup>-/-</sup> mice are shown in (**f**). Data in each panel reflect the summary of  $n = 5$  mice/group with two independent experiments. Gene expression levels detected in HSV-infected WT mice are depicted for reference in panels **c**, **d**, and **f**. Abbreviations: TCID<sub>50</sub>, median tissue culture infectious dose; ND not detected, WT wild-type, *Nos2* inducible nitric oxide synthase, *Il1b* interleukin 1 $\beta$ , *Ifn* interferon, *Becn1* beclin1, *Ripk1* receptor-interacting serine/threonine-protein kinase 1, *FcRn* neonatal Fc receptor, *Irf* interferon regulatory factor, *Nfkb* nuclear factor kappa-light-chain-enhancer of activated B cells, *Rnasel* ribonuclease L, *Trim21* tripartite motif-containing protein 21, *Eif2ak2* eukaryotic translation initiation factor 2-alpha kinase 2, *Bst2* bone-marrow stromal antigen 2 (tetherin), *Tlr* toll-like receptor, *H2-K1* histocompatibility 2, K1 region (MHC class I), *Ccl2* c-c motif chemokine ligand 2

to characterize the repertoire of viral proteins recognized by HSV-1 0 $\Delta$ NLS antiserum. Antiserum from HSV-1 0 $\Delta$ NLS-vaccinated WT mice selectively and reproducibly immunoprecipitated twenty HSV-1 proteins from infected cell lysates (Figs. 6a, b). These targets included non-structural infected cell proteins (ICPs), virion surface glycoproteins, and sequestered proteins from the virion tegument and capsid (Fig. 6b). Viral proteins were identified by matching derivative tryptic peptides to the HSV-1 reference proteome as described in the supplementary methods. Envelope glycoproteins only represented 26% of all viral proteins immunoprecipitated with HSV-1 0 $\Delta$ NLS antiserum based on total peptide counts. Non-structural ICPs and tegument proteins each accounted for 10% of

recognized viral proteins, and the majority of targets (53%) were identified as capsid proteins (Fig. 6b, inset). Target protein mass likely did not bias results, as no correlations were identified between protein size (kD) and matched tryptic peptide counts (Fig. 6c). Non-viral proteins identified with serum from naive and vaccinated mice likely represent Vero cell xenoantigens or contaminants. Moreover, no viral peptides were identified in serum-free preparations.

Studies of the *intraviral* "interactome" of HSV-1 have uncovered a complex array of protein-protein interaction networks.<sup>48</sup> Accordingly, it remains possible that the immunoprecipitation products detected by mass spectrometry with HSV-1 0 $\Delta$ NLS

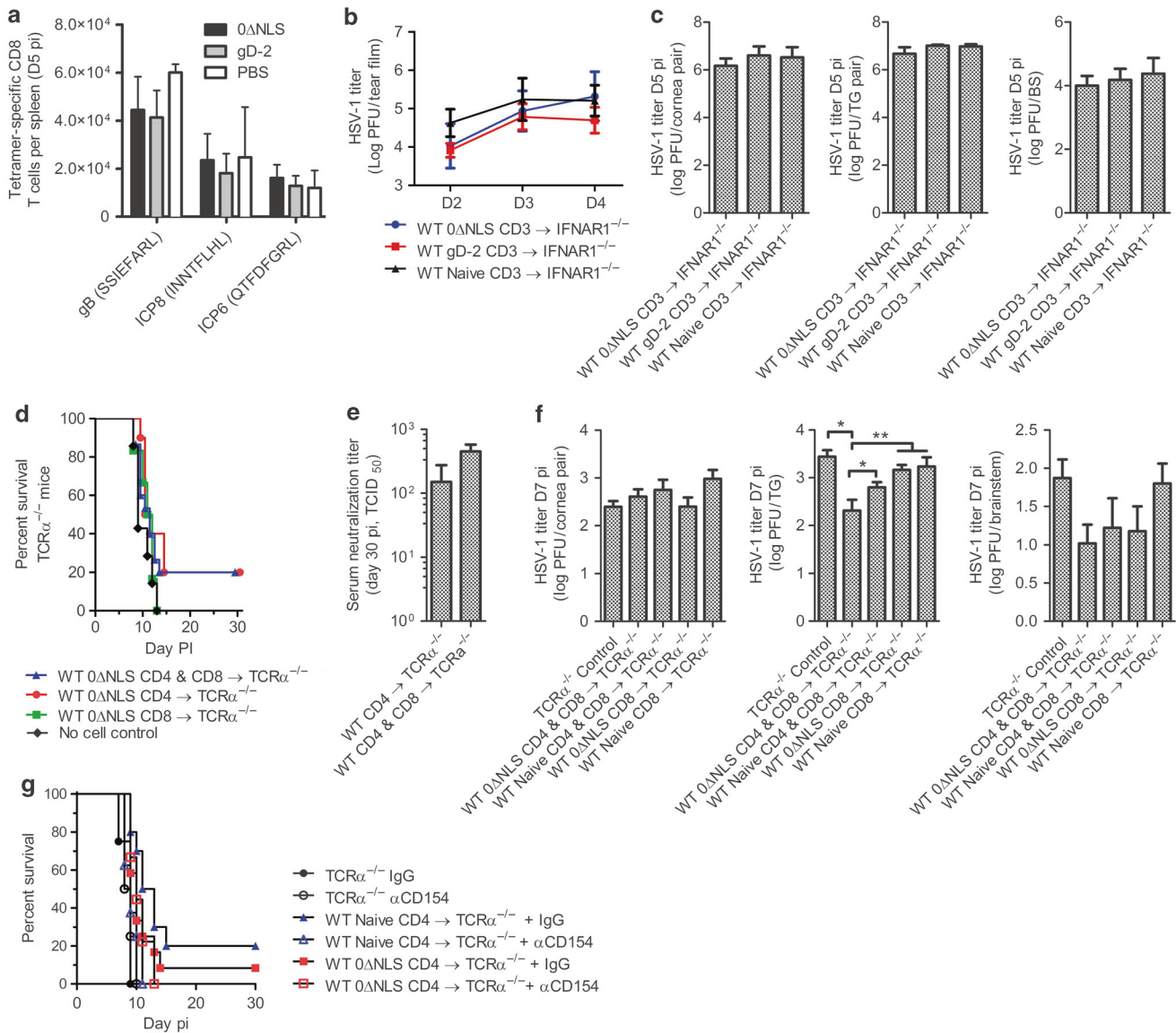


**Fig. 4** Contributions of cell-mediated immunity to prophylactic protection. **a** Flow cytometric analysis of HSV-1 specific CD8 T cells in the spleen of naive and vaccinated WT mice at day 5 p.i. based on tetramer labeling for the top three immunodominant HSV-1 epitopes in C57BL/6 mice including glycoprotein B (gB), and infected cell proteins 6/8 (ICP6/8). Antigen peptide sequences are listed parenthetically ( $n = 4$  vaccinated, 2 naive mice/group; 2 independent experiments). **b** Viral shedding in the corneas of *Ifnar1*<sup>-/-</sup> mice receiving  $1 \times 10^6$  CD3<sup>+</sup> T cells i.v. from the spleens of HSV-1 0ΔNLS-vaccinated WT mice concurrent with ocular HSV-1 infection at  $1 \times 10^3$  PFU HSV-1 McKrae per eye ( $n = 3$  mice per group, 2 independent experiments). **c** Viral titers in the corneas, TG, and brainstem of *Ifnar1*<sup>-/-</sup> mice as in (**b**). **d** Survival of *TCRα*<sup>-/-</sup> mice ocularly challenged with  $1 \times 10^4$  PFU HSV-1 McKrae/eye 7 days after adoptive transfer of  $1 \times 10^5$  CD4,  $1 \times 10^5$  CD8, or  $1 \times 10^5$  of both CD4 and CD8 T cells i.v. from the spleens of HSV-1 0ΔNLS-vaccinated WT mice ( $n = 6-15$  mice/group; 3 independent experiments). **e** Serum neutralization titers in *TCRα*<sup>-/-</sup> mice that survived ocular HSV-1 infection upon receiving T cells from HSV-1 0ΔNLS-vaccinated WT mice ( $n = 3-4$  mice/group). **f** Viral titers in the corneas, TG, and brainstem of *TCRα*<sup>-/-</sup> mice as in (**c**), with the addition of naive WT donors ( $n = 5-6$  mice/group; 2 independent experiments). **g** Survival of *TCRα*<sup>-/-</sup> mice ocularly challenged with  $1 \times 10^4$  PFU HSV-1 McKrae/eye 7 days after adoptive transfer of  $1 \times 10^5$  CD4 T cells from HSV-1 0ΔNLS-immunized or naive WT mice; *TCRα*<sup>-/-</sup> mice were treated with 250 μg anti-CD154 antibody or Rat IgG control i.p. on day 0, 3, and 6 p.i. ( $n = 8-12$  mice + T cells,  $n = 4$  no-cell controls; 3 independent experiments). Data in panels A, C, F were analyzed by one-way ANOVA with Newman-Keuls multiple comparisons tests; data in panels **b** and **e** were evaluated two-way ANOVA and Student's *T* test, respectively

antiserum contained protein-protein complexes that may have contributed to indirect 'false-positive' target identification. Nonetheless, twenty viral proteins were consistently identified in our studies despite the hundreds of possible "intraviral" protein-protein interactions confirmed for HSV-1 (Fig. 7d).<sup>48</sup> To explore whether the sequestered viral proteins we identified are probable antibody targets or indirect co-immunoprecipitation products of envelope glycoproteins, we used in silico bioinformatics to query

all primary binding partners of gB, gC, gD, and gE with HVint—an open-access HSV-1 interactome database (<http://topf-group.ismb.lon.ac.uk/hvint/>). Only 7 out of 28 confirmed non-homodimeric envelope glycoprotein-binding partners (25%) were included in our list of sequestered viral proteins identified by proteomic screening. Collectively, our data suggest that effective immunity to HSV-1 provided by prophylactic vaccination with HSV-1 0ΔNLS involves broad antibody responses against both exposed virion

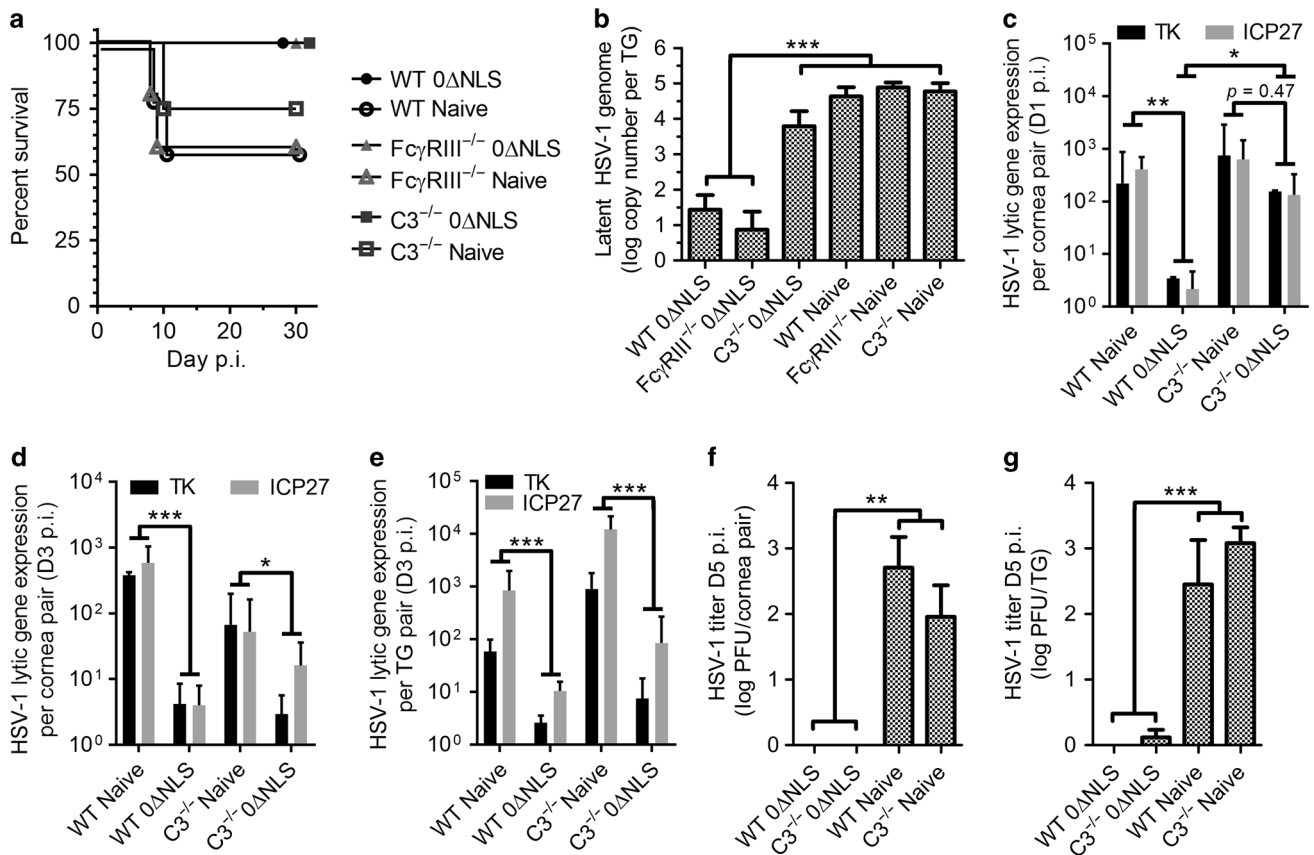


**Fig. 5** Contributions of complement C3 and Fc $\gamma$ -receptor 3 to prophylactic protection against viral latency. **a** Survival of naive and HSV-1 0 $\Delta$ NLS-vaccinated WT, Fc $\gamma$ RIII $^{-/-}$ , and C3 $^{-/-}$  mice following ocular challenge with  $1 \times 10^4$  PFU HSV-1 McKrae per eye ( $n \geq 5$  mice/group; 2 independent experiments). **b** Quantitative PCR reads of HSV-1 genome copy numbers in the trigeminal ganglia (TG) of surviving WT, Fc $\gamma$ RIII $^{-/-}$ , and C3 $^{-/-}$  mice at day 30 p.i. ( $n = 4-7$  TG per group; 2 independent experiments). **c** Viral lytic gene expression in corneas from naive and HSV-1 0 $\Delta$ NLS-vaccinated WT and C3 $^{-/-}$  mice 24 h p.i. ( $n = 2-3$  mice per group; 2 independent experiments). Viral lytic gene expression in the cornea and TG of naive and vaccinated WT and C3 $^{-/-}$  mice at day 3 p.i. ( $n = 4-5$  mice per group; 2 independent experiments). Viral lytic gene expression in panels C-E was relative to murine *beta actin* expression and normalized to tissue from uninfected WT C57BL/6 mice. Viral titers in corneas (**f**) and TG (**g**) from WT and C3 $^{-/-}$  mice at day 5 p.i. ( $n = 2-3$  mice per group; 2 independent experiments). Data in panels **b, f, g** were analyzed by one-way ANOVA with Newman-Keuls multiple comparisons tests. Data in panels **c-e** were analyzed by two-way ANOVA with Tukey's multiple comparisons tests

envelope glycoproteins and sequestered viral antigens. Moreover, our recent identification that FcRn is essential for humoral protection against ocular HSV-1 infection combined with the identification of multiple sequestered/intracellular viral protein targets herein builds a strong argument that humoral immunity against HSV-1 is not restricted to the extracellular space. While further investigation is ultimately required to determine epitope specificity and binding kinetics, our work underscores that vaccines targeting viral surface antigens alone may be insufficient for protection against HSV-1.

Prophylactic protection elicited by the HSV-1 0 $\Delta$ NLS vaccine preserves the visual axis against immunopathology and vision loss. The HSV-1 0 $\Delta$ NLS vaccine amplifies host immunity to mediate protection against HSV-1 pathogenesis, but its impact on visual health remained to be determined in C57BL/6 mice. Therefore, a comprehensive histologic and functional evaluation of corneal health was conducted to establish the protective efficacy of HSV-1 0 $\Delta$ NLS against ocular immunopathology and vision loss in WT mice. Animals were evaluated for corneal neovascularization, scarring, opacity, and sensory nerve defects at day 30 p.i. Functional visual acuity was tested by optokinetic tracking reflexes. Confocal imaging of corneolimbal buttons revealed that neovascularization was prevented in HSV-1 0 $\Delta$ NLS-immunized

mice (Fig. 7a), whereas robust hemangiogenesis and lymphangiogenesis were observed in corneas from gD-2-immunized and naive mice (Figs. 7b, c). Second harmonic generation (SHG) microscopy showed that central corneal scarring was prevented in nearly all HSV-1 0 $\Delta$ NLS-immunized mice, although corneas from gD-2-immunized and naive mice exhibited varying degrees of pathologic collagen remodeling (Figs. 7d, e). Additionally, the HSV-1 0 $\Delta$ NLS vaccine also prevented robust corneal neovascularization and fibrosis in *fnar1* $^{-/-}$  mice (Fig. S2).

Consistent with corneal neovascularization and scarring data in WT mice, non-invasive slit lamp biomicroscopy examinations revealed progressive corneal opacification in naive and gD-2-immunized mice following ocular HSV-1 challenge. In contrast, corneal clarity was preserved in HSV-1 0 $\Delta$ NLS-immunized mice (Fig. 7f). Sensory nerve deficits are another hallmark of corneal herpetic disease;<sup>49</sup> therefore, corneal sensation was measured via Cochet-Bonnet esthesiometry. No sensation loss was detected in HSV-1 0 $\Delta$ NLS-immunized mice (Fig. 7g). Comparatively, gD-2-immunized and naive mice exhibited moderate to severe sensation loss, (Fig. 7g). Multiple assessments indicate that the HSV-1 0 $\Delta$ NLS vaccine averts corneal pathology, yet preservation of functional visual acuity remained to be demonstrated. To that end, optokinetic tracking reflexes were monitored as a behavioral indicator of visual acuity. Following challenge, gD-2-immunized

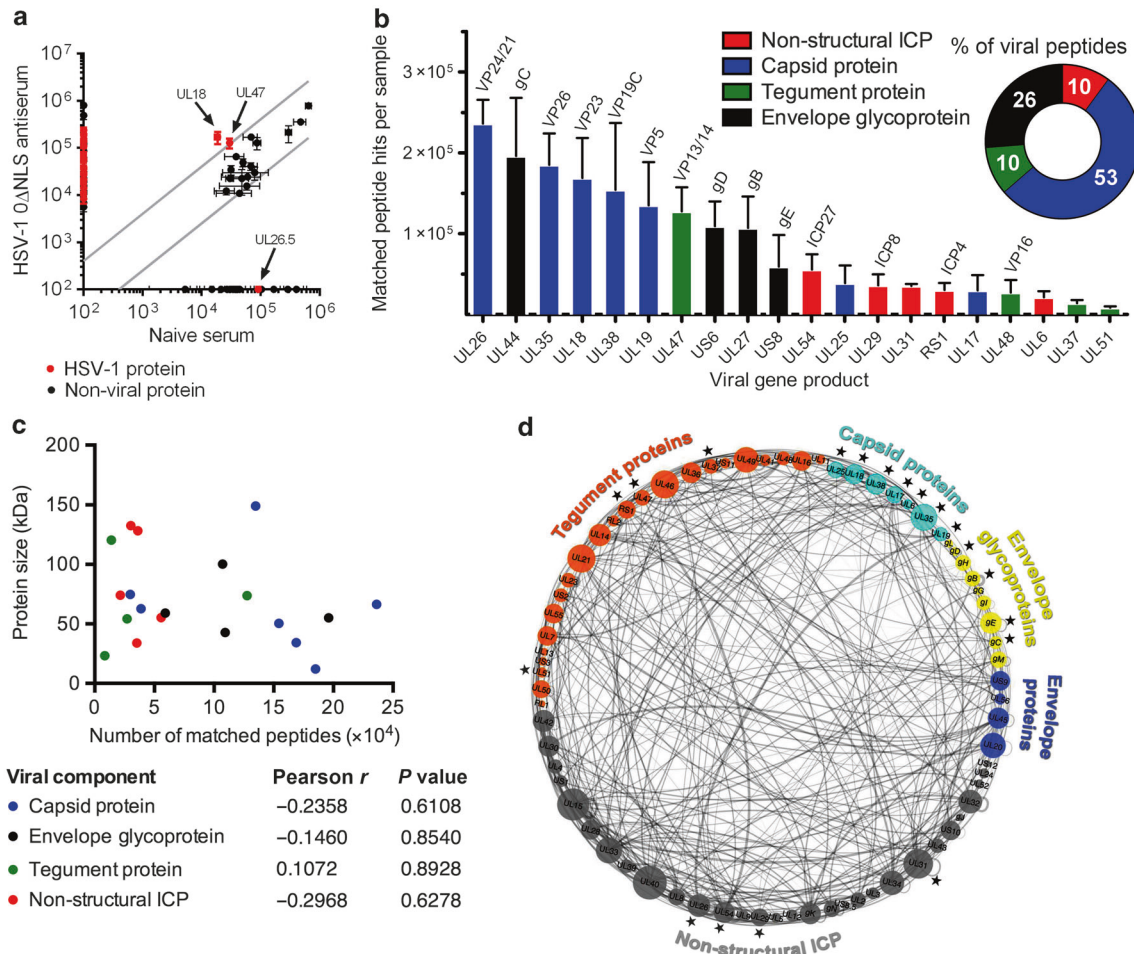


**Fig. 6** Identification of viral proteins targeted by vaccine-induced antibodies. **a** Serum from HSV-1 0ΔNLS-vaccinated and naive WT mice was utilized to immunoprecipitate proteins from HSV-1 infected Vero cell lysates. Precipitated proteins were eluted and analyzed by mass spectrometry. Virus-derived and non-viral proteins were identified by cross-referencing derivative tryptic peptide ions with a reference sequence database. Data reflect the numbers of matched peptides per protein derived from HSV-1 or from other sources immunoprecipitated by HSV-1 0ΔNLS antiserum and/or naive serum ( $n = 5$  serum samples/group; 3 independent experiments). Viral proteins are shown in red and non-viral proteins are shown in black. Gray lines indicate a 4-fold change in peptide abundance comparing naive and immune serum. **b** Repertoire of precipitated HSV-1-derived proteins ranked by average tryptic peptide abundance and labeled according to viral protein class (i.e., non-structural infected cell proteins (ICP), red; capsid, blue; tegument, green or envelope glycoprotein, black). Inset pie chart shows the percentage of viral protein targets by class based on the average number of matched viral peptides ( $n = 5$  serum samples/group; 3 independent experiments). **c** Pearson correlation analysis was performed on viral targets immunoprecipitated by HSV-1 0ΔNLS antiserum to determine the relationship between the average numbers of matched tryptic peptides and the size of each parent viral protein (kD). Molecular weights were queried from the HSV-1 reference proteome accessible at <http://www.uniprot.org> online. Each data point reflects a viral target protein identified from  $n \geq 2$  of 5 total serum samples analyzed across three independent experiments. Pearson correlation coefficients ( $r$ ) and  $p$  values were determined using GraphPad Prism. **d** Graphical representation of the intraviral interactome among the subdivisions of viral proteins. Target proteins identified in the proteomic screen are labeled with a black star. Internal lines show confirmed interactions between HSV-1 proteins. Figure was modified from its original format (Ashford et al. Mol. Cell. Proteomics. 2016 Sep; 15: 2939–2953)<sup>48</sup> and reproduced via creative commons 4.0 attribution licensing (<http://creativecommons.org/licenses/by/4.0/>)

and naive mice sustained significant vision loss (Fig. 7h). However, visual acuity was preserved in HSV-1 0ΔNLS-immunized mice (Fig. 7h). In summary, prophylactic protection elicited by the HSV-1 0ΔNLS vaccine protects not only against HSV-1 pathogenesis but also against resultant inflammatory tissue pathology and visual morbidity.

## DISCUSSION

Our study demonstrates the prophylactic efficacy of HSV-1 0ΔNLS, a live-attenuated vaccine, against ocular HSV-1 pathogenesis and pathology in C57BL/6 mice. Using multiple approaches, we observed that the HSV-1 0ΔNLS vaccine drives a robust T-dependent humoral immune response against a broad

repertoire of HSV-1-encoded proteins to inhibit viral neuroinvasion and latency. While the antiviral IFN $\alpha$ / $\beta$  signaling pathway and Fc $\gamma$ RIII were dispensable for protection, efficacy was diminished in the absence of complement C3. A direct contribution of T cells as antiviral effectors was not observed in our adoptive transfer studies. However, in the case of HSV-1 0ΔNLS, the dominance of antibody-mediated viral clearance may influence the local cytokine milieu to restrain antigen presenting cell activation and ‘inappropriate T cell help’ by favoring regulatory T cell stability and preventing the progression of herpetic keratitis by Th1/Th17-polarized CD4 T cells.<sup>50–52</sup> Thorough evaluation of the visual axis is of utmost importance when assessing vaccines for common ocular infections. The concern surrounding this element is underscored by the fact that clinical trials for HSV vaccines have

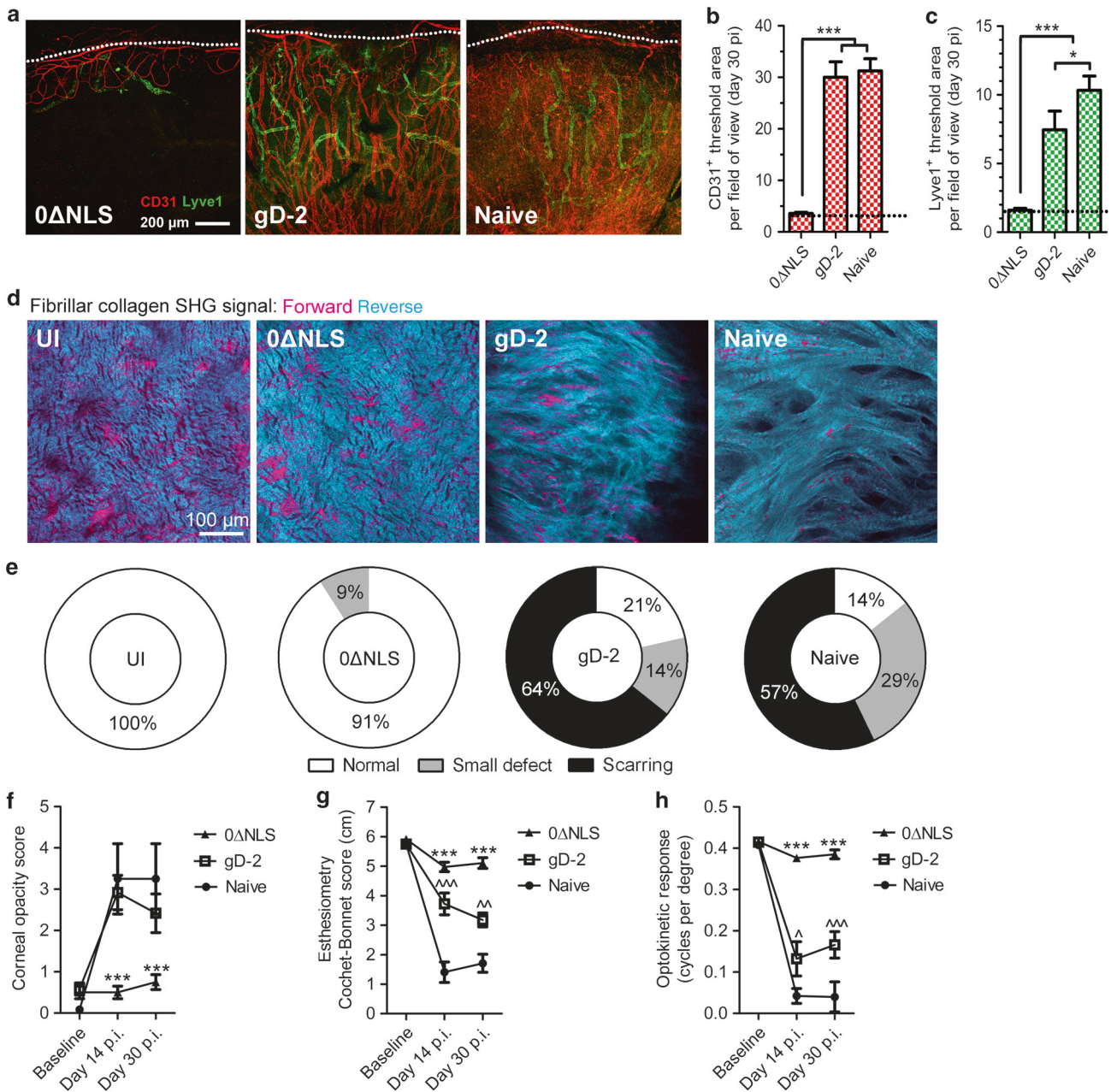


**Fig. 7** Impact of vaccination on the visual axis. Corneas of naive and vaccinated WT mice were evaluated for signs of pathology at day 30 following ocular infection with  $1 \times 10^4$  PFU HSV-1 McKrae/eye. **a** Corneal neovascularization, shown by confocal imaging of CD31 + blood vessels and Lyve1 + lymphatic vessels extending from the normally vascularized peri-corneal limbus (dotted lines, top) towards the normally avascular central cornea (bottom) in corneal whole mounts. Corneal hemangiogenesis (**b**) and lymphangiogenesis (**c**) were quantified by corneal area positive for CD31 and Lyve1 labeling per field of view; dotted lines reflect area positive for in healthy uninfected corneas (aggregate data from corneal quadrants of  $n = 4-10$  mice/group; 2-3 independent experiments). **d** Representative multi-photon microscopy images showing second harmonic generation (SHG) signal of fibrillar collagen in the central corneas of naive and vaccinated mice at day 30 p.i. **e** Qualitative analysis of corneal SHG signals from mice as in (D) showing degrees of collagen remodeling/scarring ( $n = 8-15$  corneas from challenged mice,  $n = 4$  healthy control corneas; 2 independent experiments). Longitudinal tracking of corneal opacity (**f**), sensory nerve function (**g**), and visual acuity (**h**) in naive and immunized mice following ocular HSV-1 challenge ( $n \geq 4-12$  mice/group/time). Data in panels **b** and **c** were evaluated by one-way ANOVA with Newman-Keuls multiple comparisons tests; data in panels **f-h** were evaluated by two-way ANOVA with Bonferroni post-tests. For panels **f-h**, \* signifies differences between 0ΔNLS and gD-2/naive; ^ reflects differences between gD-2 and naive

specifically excluded patients with a history of ocular HSV-1 involvement.<sup>11</sup> Furthermore, our comprehensive analysis of the visual axis shows that prophylactic vaccination with HSV-1 0ΔNLS effectively controls HSV-1 pathogenesis without eliciting ocular pathology or visual morbidity. These findings are unparalleled by previous studies.

For widespread clinical efficacy, the ideal prophylactic HSV-1 vaccine must preclude the establishment of neuronal latency to mitigate the threat of reactivation-associated shedding, horizontal transmission, and ultimately ocular disease. The exact mechanisms underlying the regulation of HSV-1 latency are not fully understood, yet current knowledge of this process stems from in vitro

studies or primary infection in immunologically naive animals.<sup>35</sup> Furthermore, the total amount of latent virus in the TG correlates with reactivation risk in animal models.<sup>12,24</sup> Recent evidence of lytic gene expression during latency challenges the longstanding stable quiescence model of HSV-1 latency.<sup>13</sup> In immunologically naive animals, HSV-specific CD8<sup>+</sup> T cells generated *after* neuronal infection promote resolution of the lytic cycle and govern neuronal latency.<sup>40</sup> In the absence of prophylactic protection, persistent viral lytic gene activity in neurons during latency contributes to functional exhaustion of tissue-resident antiviral T cells.<sup>53,54</sup> In contrast, our data show that *prophylactic* humoral immunity blocks productive infection of neurons and significantly limits the establishment of viral latency following ocular challenge. The cornea is the most densely innervated tissue in the body and a prime target for HSV-1 replication.<sup>55</sup> Accordingly, a vaccine such as HSV-1 0ΔNLS that demonstrably curbs HSV-1 neuroinvasion following corneal infection with a high-titer inoculum as demonstrated herein offers hope in the quest to prevent HSV-1 infection in other sites supplied with fewer sensory nerve fibers.

Although the amount of latent virus in animals vaccinated with HSV-1 0ΔNLS is minimal relative to naive controls, latent virus presents an important safety concern for reactivation potential. Our evidence collectively suggests that the establishment of neuronal latency occurs independent of lytic gene expression (ICP0) in the TG of vaccinated animals. This may reflect delivery of HSV-1 DNA into sensory nerve fibers in peripheral sites without viral replication in neurons (i.e., non-productive infection, the minimal requirement for latency establishment).<sup>35</sup> Accumulating evidence demonstrates the ability of UV-inactivated herpesviruses (HCMV) to deliver viral DNA to cells independent of productive replication—yet the stability of the viral genome is transient in this model.<sup>56,57</sup> Alternatively, productively infected neurons may be cleared in animals vaccinated with HSV-10ΔNLS, but this occurs without obvious sensory deficits. Whether prophylactic protection affects cell-mediated immune responses in neuronal ganglia or HSV-1 reactivation potential remains to be determined. From a clinical perspective, whether a vaccine must completely prevent establishment of herpesvirus latency to be protective against clinical disease is debatable. Longitudinal clinical data show that varicella zoster virus (VZV) reactivation (i.e., “shingles”) is rare in vaccinated children.<sup>58,59</sup> Moreover, vaccine-induced antibody is the clinical correlate of prophylactic protection against VZV.<sup>60</sup>

Other immunologic aspects requisite for an optimally efficacious prophylactic HSV-1 vaccine remain to be explored. The partial reduction in viral titers in the tear film and TG of HSV-1 0ΔNLS-immunized μMT mice may be attributable to HSV-specific CD4 T cell enhancement of NK cell activity.<sup>61,62</sup> Furthermore, the necessity of CD4 T cells and CD154 for animal survival may also implicate follicular helper T cells (T<sub>FH</sub>) as central players in humoral defense against HSV-1.<sup>63</sup> Whether HSV-1 modulates the function of T<sub>FH</sub> cells as an immunoevasion strategy during primary infection in naive hosts is currently unknown. Evidence suggests that strong type 1 IFN responses limit induction of T<sub>FH</sub> responses and antibody production during systemic infections.<sup>64</sup> Likewise, whether altered T<sub>FH</sub> responses to HSV-1 in naturally infected or prophylactically vaccinated subjects extrapolate into differences in antibody repertoire will need to be determined. Other investigators have focused on prophylactically boosting tissue-resident memory T cell responses to HSV-1 through “prime and pull” approaches in animal models.<sup>37,39</sup> However, the efficacy of prime and pull against viral dissemination following ocular infection has not been characterized, and the absence of iatrogenic corneal pathology was not convincingly demonstrated. Recruiting T cells to the cornea in an effort to control HSV-1 may not be clinically suitable, as T cells are associated with tissue pathology in HSV keratitis, and progression of inflammatory disease occurs independently of active viral infection.<sup>65,66</sup>

Other facets of prophylactic immunity to HSV also require further exploration, such as whether the mechanism of humoral protection observed in the eye involving FcRn and complement C3 is applicable to other sites of mucosal or cutaneous exposure where FcγRIII is reportedly essential.<sup>22,67</sup> The protective effect of human gammaglobulin against neurological disease caused by HSV-1 was identified in the mid-20<sup>th</sup> century using *in vitro* virus neutralization and passive immunization in mice,<sup>68</sup> yet the mechanistic role of antibody against HSV-1-associated neurological disease has been debated since the mid 1970's.<sup>69–71</sup> Nonetheless, recent published data confirm that antibody is an essential host countermeasure against HSV-1 neurodissemination.<sup>21,22,72</sup>

Most HSV vaccines to date have focused on gB and gD protein subunits,<sup>11,47</sup> however, generating antibody responses against sequestered or non-dominant antigens has not been widely considered as a viable strategy until recently.<sup>67,73</sup> We have previously demonstrated that the gD-2 vaccine mediates partial protection against ocular HSV-1 challenge in outbred CD-1 mice. However, the gD-2 subunit vaccine failed to promote antibody responses or protective effects in C57BL/6 mice. Notably, protection against HSV-1 infection mediated by a similar subunit vaccine in humans correlated with anti-gD-2 antibody titers.<sup>74</sup>

Effective humoral protection against HSV-1 may involve targeting more than neutralizing exposed surface glycoproteins. Of significant interest is the fact that one of the dominant antigens targeted by HSV-1 0ΔNLS antiserum is HSV-1 gC, a surface glycoprotein that functions to inhibit complement activation.<sup>75</sup> Of equal interest is the observation that a large component of the humoral defense against HSV-1 elicited by prophylactic vaccination with HSV-1 0ΔNLS is targeted against the virion capsid. Future work is necessary to determine if antibody-bound capsids are capable of successfully delivering viral DNA to the nucleus. One caveat to our approach is that the cell lysis buffer utilized may not have dissociated individual capsid protein-protein interactions; nevertheless, a constituent (or constituents) from the capsid were immunoprecipitated by HSV-1 0ΔNLS antiserum. In addition, the UL37 tegument protein functionally associated with neuronal retrograde transport was also recognized by antiserum.<sup>76</sup> Accordingly, it is plausible that intracellular antibody inhibits the function of various viral tegument or transactivator proteins such as ICP4 to reduce infectivity or reactivation potential. It remains to be determined if the ability of antibody to engage sequestered/intracellular antigens is restricted to particular intracellular compartments—and whether intracellular antibody compartmentalization is unique in various cell types. The implications of intracellular humoral protection may shed light on the long-standing efficacy of many other live-attenuated viral vaccines.<sup>60</sup>

Using mass spectrometry to evaluate the repertoire of viral targets recognized by antibodies following immunization with a live-attenuated vaccine encompassing nearly all of the viral proteome may prove to be an effective approach to identify the most relevant antigens for next-generation prophylactic vaccine development. Moreover, identification of sequestered and presumably intracellular proteins that are targeted by antibody supports our recent findings that FcRn arbitrates viral clearance in the cornea by mediating intracellular transcytosis of IgG through the corneal epithelium.<sup>22</sup> Whether effective humoral immunity against HSV-1 can be achieved through targeting a small number of critical antigens or whether a broad repertoire of exposed and sequestered antigens is necessary to achieve clinically meaningful protection in a genetically diverse human population remains to be determined. Nonetheless, the identification of sequestered and intracellular viral proteins as antibody targets reflects a new concept in the pursuit of an effective HSV-1 vaccine. Advancing these concepts forward will require continued investment in improving adjuvants to mediate effective and sustained

protection with subunit cocktail vaccines<sup>77,78</sup> or increasing acceptance of novel, live-attenuated viruses for clinical utilization.

## ACKNOWLEDGEMENTS

We expressly thank Min Zheng, Jeremy Jinkins, Meghan Carr, Renee Sallack, and Pouriska Kivanany for technical assistance as well as Todd Margolis for reviewing the manuscript. We thank the Laboratory for Molecular Biology and Cytometry Research at OUHSC for use of the Core Facility, which provided proteomic services. We acknowledge the following individuals/entities for providing material resources: Edward Gershburg, recombinant glycoprotein D; Helen Rosenberg, original *Ifnar1*<sup>-/-</sup> breeders; Brian Gebhardt, original stock of HSV-1 McKrae; Stacey Efstathiou, recombinant HSV-1 SC16 ICP0-Cre virus; Rational Vaccines, Inc., live-attenuated HSV-1 0ΔNLS vaccine. We dedicate this work to our close colleague and friend, William Halford, who passed away 22 June, 2017.

## FUNDING

This work was supported by National Institutes of Health Grants R01 AI021238, P30 EY021725, T32 EY023202, and a seed grant from the Presbyterian Health Foundation. V.H.S. was supported in part by the National Institute of General Medical Sciences grant P20 GM103447. Additional support was provided by an unrestricted grant from Research to Prevent Blindness. The content of the manuscript is solely the responsibility of the authors and does not necessarily represent the official views of the National Institutes of Health or its subsidiaries.

## AUTHOR CONTRIBUTIONS

D.J.R. planned and conducted experiments, performed data analysis, generated figures, and composed the manuscript; J.F.H. scored corneal opacity (Fig. 7f); C.M.L. and A.M.R. evaluated optokinetic-tracking responses (Fig. 7h); V.H.S. performed all mass spectrometry (Fig. 6); D.M.R. assisted with SHG microscopy (Fig. 7d, Fig. S2); D.J. J.C. performed experiments, edited the manuscript, and supervised all work.

## DATA AVAILABILITY

The HSV-1 0ΔNLS vaccine is under US patent protection and distribution would be at the discretion of Rational Vaccines, Inc. Acquisition of the other non-commercial materials would require contact with the original sources listed above.

## ADDITIONAL INFORMATION

The online version of this article (<https://doi.org/10.1038/s41385-019-0131-y>) contains supplementary material, which is available to authorized users.

**Competing interests:** D.J.J.C. is an advisory board member of Rational Vaccines, Inc., which has licensed U.S. patents 7785605 and 8802109 involving ICP0-mutant herpesviruses. The remaining authors declare no competing interests.

**Publisher's note:** Springer Nature remains neutral with regard to jurisdictional claims in published maps and institutional affiliations.

## REFERENCES

- Foulsham, W., Coco, G., Amouzegar, A., Chauhan, S. K. & Dana, R. When clarity is crucial: regulating ocular surface immunity. *Trends Immunol.* (2017). <https://doi.org/10.1016/j.it.2017.11.007>
- Galletti, J. G., Guzmán, M. & Giordano, M. N. Mucosal immune tolerance at the ocular surface in health and disease. *Immunology* **150**, 397–407 (2017).
- Taylor, A. W. & Ng, T. F. Negative regulators that mediate ocular immune privilege. *J. Leukoc. Biol.* (2018). <https://doi.org/10.1002/JLB.3MIR0817-337R>
- Niederhorn, J. Y. Cornea: window to ocular immunology. *Curr. Immunol. Rev.* **7**, 328–335 (2011).
- Stepp, M. A. et al. Wounding the cornea to learn how it heals. *Exp. Eye Res.* **121**, 178–193 (2014).
- Benítez-Del-Castillo, J. et al. Visual acuity and quality of life in dry eye disease: Proceedings of the OCEAN group meeting. *Ocul. Surf.* **15**, 169–178 (2017).
- Henry, C., Palioura, S., Amescua, G. & Alfonso, E. Role of steroids in the treatment of bacterial keratitis. *Clin. Ophthalmol.* (2016). <https://doi.org/10.2147/OPHT.580411>.

- Rajasagi, N. K. & Rouse, B. T. Application of our understanding of pathogenesis of herpetic stromal keratitis for novel therapy. *Microbes Infect.* (2018). <https://doi.org/10.1016/j.micinf.2017.12.014>
- Farooq, A. V. & Shukla, D. Herpes simplex epithelial and stromal keratitis: an epidemiologic update. *Surv. Ophthalmol.* **57**, 448–462 (2012).
- Belshe, R. B. et al. Efficacy results of a trial of a herpes simplex vaccine. *N. Engl. J. Med.* **366**, 34–43 (2012).
- Royer, D. J., Cohen, A. W. & Carr, D. J. The current state of vaccine development for ocular HSV-1 infection. *Expert. Rev. Ophthalmol.* **10**, 113–126 (2015).
- Sawtell, N. M., Poon, D. K., Tansky, C. S. & Thompson, R. L. The latent herpes simplex virus type 1 genome copy number in individual neurons is virus strain specific and correlates with reactivation. *J. Virol.* **72**, 5343–5350 (1998).
- Ma, J. Z., Russell, T. A., Spelman, T., Carbone, F. R. & Tschärke, D. C. Lytic gene expression is frequent in HSV-1 latent infection and correlates with the engagement of a cell-intrinsic transcriptional response. *PLoS. Pathog.* **10**, e1004237 (2014).
- Remeijer, L. et al. Prevalence and clinical consequences of herpes simplex virus type 1 DNA in human cornea tissues. *J. Infect. Dis.* **200**, 11–19 (2009).
- Jaishankar, D., Bührman, J. S., Valyi-Nagy, T., Gemeinhart, R. A. & Shukla, D. Extended release of an anti-heparan sulfate peptide from a contact lens suppresses corneal herpes simplex virus-1 infection. *Investig. Ophthalmology Vis. Sci.* **57**, 169 (2016).
- Birkmann, A. & Zimmermann, H. Drugs in development for herpes simplex and varicella zoster virus. *Clin. Pharmacol. Ther.* **102**, 30–32 (2017).
- Jaishankar, D. et al. An off-target effect of BX795 blocks herpes simplex virus type 1 infection of the eye. *Sci. Transl. Med.* **10**, eaan5861 (2018).
- Khan, A. A. et al. Therapeutic immunization with a mixture of herpes simplex virus 1 glycoprotein D-derived “asymptomatic” human CD8 + T-cell epitopes decreases spontaneous ocular shedding in latently infected HLA transgenic rabbits: association with low frequency of local PD-1 + TIM-3 + CD8 + exhausted T cells. *J. Virol.* **89**, 6619–6632 (2015).
- Johnston, C., Gottlieb, S. L. & Wald, A. Status of vaccine research and development of vaccines for herpes simplex virus. *Vaccine* **34**, 2948–2952 (2016).
- Khan, A. A. et al. Bolstering the number and function of HSV-1-specific CD8 + effector memory T cells and tissue-resident memory T cells in latently infected trigeminal ganglia reduces recurrent ocular herpes infection and disease. *J. Immunol.* **199**, 186–203 (2017).
- Royer, D. J. et al. A highly efficacious herpes simplex virus 1 vaccine blocks viral pathogenesis and prevents corneal immunopathology via humoral immunity. *J. Virol.* **90**, 5514–5529 (2016).
- Royer, D. J., Carr, M. M., Gurung, H. R., Halford, W. P. & Carr, D. J. J. The neonatal Fc receptor and complement fixation facilitate prophylactic vaccine-mediated humoral protection against viral infection in the ocular mucosa. *J. Immunol.* **199**, 1898–1911 (2017).
- Royer, D. J., Carr, M. M., Chucair-Elliott, A. J., Halford, W. P. & Carr, D. J. J. Impact of type 1 interferon on the safety and immunogenicity of an experimental live-attenuated herpes simplex virus type 1 vaccine in mice. *J. Virol.* **91**, e02342–16 (2017).
- Proenca, J. T., Coleman, H. M., Connor, V., Winton, D. J. & Efstathiou, S. A historical analysis of herpes simplex virus promoter activation in vivo reveals distinct populations of latently infected neurons. *J. Gen. Virol.* **89**, 2965–2974 (2008).
- Royer, D. J., Zheng, M., Conrady, C. D. & Carr, D. J. J. Granulocytes in ocular HSV-1 infection: opposing roles of mast cells and neutrophils. *Invest. Ophthalmol. Vis. Sci.* **56**, 3763–3775 (2015).
- Robertson, D. M., Rogers, N. A., Petroll, W. M. & Zhu, M. Second harmonic generation imaging of corneal stroma after infection by *Pseudomonas aeruginosa*. *Sci. Rep.* **7**, 46116 (2017).
- Larabee, C. M. et al. Myelin-specific Th17 cells induce severe relapsing optic neuritis with irreversible loss of retinal ganglion cells in C57BL/6 mice. *Mol. Vis.* **22**, 332–341 (2016).
- Wiśniewski, J. R., Zougman, A., Nagaraj, N. & Mann, M. Universal sample preparation method for proteome analysis. *Nat. Methods* **6**, 359–362 (2009).
- Awasthi, S., Belshe, R. B. & Friedman, H. M. Better neutralization of herpes simplex virus type 1 (HSV-1) than HSV-2 by antibody from recipients of GlaxoSmithKline HSV-2 glycoprotein D2 subunit vaccine. *J. Infect. Dis.* **210**, 571–575 (2014).
- Austin, B. A., James, C., Silverman, R. H. & Carr, D. J. J. Critical role for the oligoadenylate synthetase/RNase L pathway in response to IFN-beta during acute ocular herpes simplex virus type 1 infection. *J. Immunol.* **175**, 1100–1106 (2005).
- Conrady, C. D., Thapa, M., Wuest, T. & Carr, D. J. J. Loss of mandibular lymph node integrity is associated with an increase in sensitivity to HSV-1 infection in CD118-deficient mice. *J. Immunol.* **182**, 3678–3687 (2009).
- Royer, D. J. & Carr, D. J. J. A STING-dependent innate-sensing pathway mediates resistance to corneal HSV-1 infection via upregulation of the antiviral effector tetherin. *Mucosal Immunol.* **9**, 1065–1075 (2016).

33. Rosato, P. C. et al. Neuronal IFN signaling is dispensable for the establishment of HSV-1 latency. *Virology* **497**, 323–327 (2016).
34. Leib, D. A. et al. Immediate-early regulatory gene mutants define different stages in the establishment and reactivation of herpes simplex virus latency. *J. Virol.* **63**, 759–768 (1989).
35. Nicoll, M. P., Proença, J. T. & Efstathiou, S. The molecular basis of herpes simplex virus latency. *FEMS Microbiol. Rev.* **36**, 684–705 (2012).
36. McEwan, W. A. et al. Intracellular antibody-bound pathogens stimulate immune signaling via the Fc receptor TRIM21. *Nat. Immunol.* **14**, 327–336 (2013).
37. Shin, H. & Iwasaki, A. A vaccine strategy that protects against genital herpes by establishing local memory T cells. *Nature* **491**, 463–467 (2012).
38. Srivastava, R. et al. A herpes simplex virus type 1 human asymptomatic CD8 + T-cell epitopes-based vaccine protects against ocular herpes in a "humanized" HLA transgenic rabbit model. *Invest. Ophthalmol. Vis. Sci.* **56**, 4013–4028 (2015).
39. Khan, A. A. et al. Human asymptomatic epitope peptide/CXCL10-based prime/pull vaccine induces herpes simplex virus-specific gamma interferon-positive CD107 + CD8 + T cells that infiltrate the corneas and trigeminal ganglia of humanized HLA transgenic rabbits and protect against ocular herpes challenge. *J. Virol.* **92**, e00535–18 (2018).
40. Knickelbein, J. E. et al. Noncytotoxic lytic granule-mediated CD8 + T cell inhibition of HSV-1 reactivation from neuronal latency. *Science* **322**, 268–271 (2008).
41. St Leger, A. J., Peters, B., Sidney, J., Sette, A. & Hendricks, R. L. Defining the herpes simplex virus-specific CD8 + T cell repertoire in C57BL/6 mice. *J. Immunol.* **186**, 3927–3933 (2011).
42. Russell, R. G., Nasisse, M. P., Larsen, H. S. & Rouse, B. T. Role of T-lymphocytes in the pathogenesis of herpetic stromal keratitis. *Invest. Ophthalmol. Vis. Sci.* **25**, 938–944 (1984).
43. Hendricks, R. L. & Tumpey, T. M. Contribution of virus and immune factors to herpes simplex virus type 1-induced corneal pathology. *Invest. Ophthalmol. Vis. Sci.* **31**, 1929–1939 (1990).
44. Koelle, D. M. et al. Tegument-specific, virus-reactive CD4 T cells localize to the cornea in herpes simplex virus interstitial keratitis in humans. *J. Virol.* **74**, 10930–10938 (2000).
45. Royer, D. J., Conrady, C. D. & Carr, D. J. J. Herpesvirus-associated lymphadenitis distorts fibroblastic reticular cell microarchitecture and attenuates CD8 T cell responses to neurotropic infection in mice lacking the STING-IFN $\alpha$ / $\beta$  defense pathways. *J. Immunol.* **197**, 2338–2352 (2016).
46. Crotty, S. A brief history of T cell help to B cells. *Nat. Rev. Immunol.* **15**, 185–189 (2015).
47. Halford, W. P. Antigenic breadth: a missing ingredient in HSV-2 subunit vaccines? *Expert. Rev. Vaccin.* **13**, 691–710 (2014).
48. Ashford, P. et al. HVint: a strategy for identifying novel protein-protein interactions in herpes simplex virus type 1. *Mol. Cell. Proteom.* **15**, 2939–2953 (2016).
49. Hamrah, P. et al. Corneal sensation and subbasal nerve alterations in patients with herpes simplex keratitis. *Ophthalmology* **117**, 1930–1936 (2010).
50. Bhela, S. et al. The plasticity and stability of regulatory T cells during viral-induced inflammatory lesions. *J. Immunol.* **199**, 1342–1352 (2017).
51. Homann, B. & Gill, R. G. To help and help not. *Nat. Immunol.* **5**, 878–880 (2004).
52. Recher, M. et al. Deliberate removal of T cell help improves virus-neutralizing antibody production. *Nat. Immunol.* **5**, 934–942 (2004).
53. Russell, T. A. & Tschärke, D. C. Lytic promoters express protein during herpes simplex virus latency. *PLoS. Pathog.* **12**, e1005729 (2016).
54. Menendez, C. M., Jenkins, J. K. & Carr, D. J. J. Resident T cells are unable to control herpes simplex virus-1 activity in the brain ependymal region during latency. *J. Immunol.* **197**, 1262–1275 (2016).
55. Shaheen, B. S., Bakir, M. & Jain, S. Corneal nerves in health and disease. *Surv. Ophthalmol.* **59**, 263–285 (2014).
56. Duan, Y.-L. et al. Maintenance of large numbers of virus genomes in human cytomegalovirus-infected T98G glioblastoma cells. *J. Virol.* **88**, 3861–3873 (2014).
57. Arcangeletti, M.-C. et al. Human cytomegalovirus reactivation from latency: validation of a "switch" model in vitro. *Virology* **13**, 179 (2016).
58. Tseng, H. F., Smith, N., Marcy, S. M., Sy, L. S. & Jacobsen, S. J. Incidence of herpes zoster among children vaccinated with varicella vaccine in a prepaid health care plan in the United States, 2002–2008. *Pediatr. Infect. Dis. J.* **28**, 1069–1072 (2009).
59. Kawai, K., Yawn, B. P., Wollan, P. & Harpaz, R. Increasing incidence of herpes zoster over a 60-year period from a population-based study. *Clin. Infect. Dis.* **63**, 221–226 (2016).
60. Plotkin, S. A. Correlates of protection induced by vaccination. *Clin. Vaccin. Immunol.* **17**, 1055–1065 (2010).
61. Jost, S. et al. CD4 + T-cell help enhances NK cell function following therapeutic HIV-1 vaccination. *J. Virol.* **88**, 8349–8354 (2014).
62. Cerwenka, A. & Lanier, L. L. Natural killer cell memory in infection, inflammation and cancer. *Nat. Rev. Immunol.* **16**, 112–123 (2016).
63. Zaretsky, A. G. et al. T follicular helper cells differentiate from Th2 cells in response to helminth antigens. *J. Exp. Med.* **206**, 991–999 (2009).
64. Zander, R. A. et al. Type I interferons induce T regulatory 1 responses and restrict humoral immunity during experimental malaria. *PLoS. Pathog.* **12**, e1005945 (2016).
65. Chentoufi, A. A. & Benmohamed, L. Mucosal herpes immunity and immunopathology to ocular and genital herpes simplex virus infections. *Clin. Dev. Immunol.* **2012**, 149135 (2012).
66. Gurung, H. R., Carr, M. M., Bryant, K., Chucair-Elliott, A. J. & Carr, D. J. Fibroblast growth factor-2 drives and maintains progressive corneal neovascularization following HSV-1 infection. *Mucosal Immunol.* **11**, 172–185 (2018).
67. Petro, C. et al. Herpes simplex type 2 virus deleted in glycoprotein D protects against vaginal, skin and neural disease. *eLife* **4**, e06054 (2015).
68. Cheever, F. S. & Daikos, G. Studies of the protective effect of gamma globulin against herpes simplex infections in mice. *J. Immunol.* **65**, 135–141 (1950).
69. Baron, S., Worthington, M. G., Williams, J. & Gaines, J. W. Postexposure serum prophylaxis of neonatal herpes simplex virus infection of mice. *Nature* **261**, 505–506 (1976).
70. Davis, W. B., Taylor, J. A. & Oakes, J. E. Ocular infection with herpes simplex virus type 1: prevention of acute herpetic encephalitis by systemic administration of virus-specific antibody. *J. Infect. Dis.* **140**, 534–540 (1979).
71. Dix, R. D., Pereira, L. & Baringer, J. R. Use of monoclonal antibody directed against herpes simplex virus glycoproteins to protect mice against acute virus-induced neurological disease. *Infect. Immun.* **34**, 192–199 (1981).
72. Jiang, Y. et al. Maternal antiviral immunoglobulin accumulates in neural tissue of neonates to prevent HSV neurological disease. *mBio.* **8**, e00678–17 (2017).
73. Geltz, J. J., Gershburg, E. & Halford, W. P. Herpes simplex virus 2 (HSV-2) infected cell proteins are among the most dominant antigens of a live-attenuated HSV-2 vaccine. *PLoS. One.* **10**, e0116091 (2015).
74. Belshe, R. B. et al. Correlate of immune protection against HSV-1 genital disease in vaccinated women. *J. Infect. Dis.* **209**, 828–836 (2014).
75. Fries, L. F. et al. Glycoprotein C of herpes simplex virus 1 is an inhibitor of the complement cascade. *J. Immunol.* **137**, 1636–1641 (1986).
76. Richards, A. L. et al. The pUL37 tegument protein guides alpha-herpesvirus retrograde axonal transport to promote neuroinvasion. *PLoS. Pathog.* **13**, e1006741 (2017).
77. Lopes, P. P. et al. Laser adjuvant-assisted peptide vaccine promotes skin mobilization of dendritic cells and enhances protective CD8 + T<sub>EM</sub> and T<sub>RM</sub> cell responses against herpes infection and disease. *J. Virol.* (2018). <https://doi.org/10.1128/JVI.02156-17>
78. Moyer, T. J., Zmolek, A. C. & Irvine, D. J. Beyond antigens and adjuvants: formulating future vaccines. *J. Clin. Invest.* **126**, 799–808 (2016).



**Open Access** This article is licensed under a Creative Commons Attribution 4.0 International License, which permits use, sharing, adaptation, distribution and reproduction in any medium or format, as long as you give appropriate credit to the original author(s) and the source, provide a link to the Creative Commons license, and indicate if changes were made. The images or other third party material in this article are included in the article's Creative Commons license, unless indicated otherwise in a credit line to the material. If material is not included in the article's Creative Commons license and your intended use is not permitted by statutory regulation or exceeds the permitted use, you will need to obtain permission directly from the copyright holder. To view a copy of this license, visit <http://creativecommons.org/licenses/by/4.0/>.

© The Author(s) 2019

